Acta Crystallographica Section B
Structural Science
ISSN 0108-7681

Structure and electrical properties of the new pyrochlore-type protonic solid electrolyte $K_{0.88}Nb_2O_{7.58}H_{4.28}$

O. Smirnova,[a]* N. Kumada,[b] T. Takei,[b] Y. Yonesaki,[b] M. Yashima[c] and N. Kinomura[b]

[a]Institute for Chemical Research, Kyoto University, Uji, Kyoto-fu 611-0011, Japan, [b]Center for Crystal Science and Technology, University of Yamanashi, 7 Miyamae-Cho, Kofu 400-8511, Japan, and [c]Tokyo Institute of Technology, Nagatsuta-cho 4259-J2-61, Midori, Yokohama, 226-8502, Japan

Correspondence e-mail: smirnova@msk.kuicr.kyoto-u.ac.jp

Received 29 May 2010
Accepted 27 September 2010

Single-crystal, synchrotron powder X-ray diffraction and neutron powder diffraction studies of the novel pyrochlore-type compound with the structural formula $K_{0.88}(OH)_{0.54}H_{1.66}(H_2O)_{1.04}Nb_2O_6$ suggests that the water molecules are located in 32*e* sites, and the hydroxide ions and potassium ions are located in 16*d* sites with a significant amount of 'free' protons in 96*g* sites. The total weight loss at temperatures up to 773 K is only about 8%, suggesting the oxygen escape from 48*f* sites can be excluded and 'free' protons must be preserved in the structure. The bulk conductivity in ambient air reaches 10^{-2} S cm^{-1} at 623 K. Owing to the extended stability range and resistance to water solubility, the compound can be considered as a candidate for intermediate temperature solid-oxide fuel-cell applications.

1. Introduction

Compounds of pyrochlore-type structure are well known for their oxygen-ion-conducting (Tuller, 1992; Kramer *et al.*, 1994), alkali-cation-conducting (Fourquet *et al.*, 1979; Grins *et al.*, 1980), proton-conducting (Fourquet *et al.*, 1988; Riviere *et al.*, 1988), ion-exchange (Kumada *et al.*, 1985; Fourquet *et al.*, 1975), photocatalytic (Ikeda *et al.*, 2006; Galati *et al.*, 2008) and superconducting properties (Galati *et al.*, 2008). The pyrochlore-like structures characterized by a three-dimensional framework of corner-sharing BO_6 octahedra belong to the space group $Fd\bar{3}m$ and have cubic cells with edges approximately 10 Å long. Presently known pyrochlore-type compounds can be arranged into several structural groups: those without *A* cations; AB_2O_6, with *A* cations in 8*b* sites; classic $A_2B_2O_7$; defect $A_2B_2O_6$; and hydrated $A_2B_2O_6{\cdot}nH_2O$. A separate group includes structures where *A* and *B* cations randomly substitute for each other (Table 1). In those groups other than the AB_2O_6 type (also called the $RbCrNiF_6$ structure type), the *A* atoms are usually in 16*d* or 16*c* sites, but are sometimes shifted into higher-multiplicity positions. If two kinds of atoms with different oxidation states substitute for each other in *B* sites, *A*-deficient pyrochlores $A_xBB'O_6{\cdot}nH_2O$ can form (Table 1). The $BO_{6/2}$ lattice contains wide tunnels suitable for incorporation of large alkali cations such as potassium or rubidium, and when $x < 1$ there is enough space for intercalation of up to two water molecules per formula unit. Water-free defect pyrochlores $A_xBB'O_6$ with $x = 2$, however, are rare. Furthermore, ion exchange of *A* cations for protons and subsequent heat treatment at temperatures around 800 K can produce oxygen-deficient pyrochlores such as $K_{0.5}TaO_{2.75}$ (Kumada *et al.*, 1985) and $TaWO_{5.5}$ (Groult *et al.*, 1982). In this contribution we report the crystal structure and the thermal and electrical properties of the pyrochlore-

Table 1
Typical representatives of pyrochlore-type compounds containing potassium or niobium (tantalum).

For 48*f* or 32*e* sites the *x* coordinate is given in parentheses. Site occupancy is equal to unity whenever it is indicated to be different.

Composition	*a* (Å)	*A* sites/fraction	*B* sites/fraction	O sites (*x*)/fraction; H(D) sites (*x*)/fraction
$(TaW)O_{5.5}$[a]	10.4372 (6)	–	Ta^{+5},W^{+6} 16*c*	O 48*f*(0.31)/0.917
$D(TaW)O_6$[b]	10.4281 (1)	–	Ta^{+5},W^{+6} 16*c*	O 48*f*(0.31) D 48*f*(0.41)/0.167
KOs_2O_6[c]	10.089 (2)	K^+ 8*b*	$Os^{+5.5}$ 16*c*	O 48*f*(0.31)
$(NH_4)(NbW)O_6$[d]	10.409 (4)	NH_4^+ 8*b*	Nb^{+5},W^{+6} 16*c*	O 48*f*(0.31)
$Ca_2Nb_2O_7$[e]	10.676 (4)	Ca^{+2} 16*c*	Nb^{+5} 16*d*	O 48*f*(0.32) O 8*b*
$(CaNd)Nb_2O_7$[f]	10.437 (1)	Ca^{+2}, Nd^{+3} 16*d*	$Nb^{+4.5}$ 16*c*	O 48*f*(0.33) O 8*b*
$Ba_{0.5}HNb_2O_6{\cdot}H_2O$[g]	10.607 (5)	Ba^{+2} 16*d*/0.25	Nb^{+5} 16*c*	O 48*f*(0.31) O 8*b*
$KNbWO_6{\cdot}(D_2O)_{0.69}$[h]	10.5019 (2)	K^{+1} 32*e*(0.49)/0.25	Nb^{+5}, W^{+6} 16*c*	O 48*f*(0.31) O 32*e*(0.41)/0.17; D 96*g*/0.115
$KNbWO_6$[h]	10.3628 (2)	K^{+1} 32*e*(0.41)/0.25	Nb^{+5}, W^{+6} 16*c*	O 48*f*(0.31)
$K_{1.88}(NbW)O_6$[h]	10.5285 (1)	K^{+1} 16*d*/0.94	$Nb^{+4.12}$, W^{+6} 16*c*	O 48*f*(0.31)
$(Pb(H_2O))Nb_2O_6$[g]	10.578 (5)	Pb^{+2} 16*d*/0.5	Nb^{+5} 16*c*	O 48*f*(0.31) O 16*d*/0.5
$K_{1.17}Bi_{2.33}O_6{\cdot}(D_2O)_{0.5}$[i]	10.9431	K^{+1} 16*d*/0.585 Bi^{+3} 16*d*/0.165	Bi^{+3} 16*c*/0.105 Bi^{+5} 16*c*/0.895	O 48*f*(0.32); O 8*b*/0.15 O 32*e*(0.45)/0.2; D 96*g*/0.08
$(K_{1.14}Bi_{0.37})(Bi_{0.27}Bi_{1.73}){\cdot}(O_{4.9}\ (OH)_{1.1})(OH)_{0.8}$[j]	10.965 (1)	K^{+1}, Bi^{+3} 16*d*	Bi^{+3}, Bi^{+5} 16*c*	O 48*f*(0.32) O 32*e*(0.41)/0.2
$K_{0.88}(OH)_{0.69}H_{1.81}(H_2O)_{0.89}Nb_2O_6$[k]	10.645 (4)	K^+ 16*d*/0.44	Nb^{+5} 16*c*	O 48*f* O 16*d*/0.24; O 32*e*/0.275

References: (*a*) Groult *et al.* (1982); (*b*) Rotella *et al.* (1982); (*c*) Riviere *et al.* (1988); (*d*) Barnes *et al.* (2003); (*e*) Lewandowski *et al.* (1992); (*f*) Istomin *et al.* (1997); (*g*) Groult *et al.* (1975); (*h*) Murphy *et al.* (1986); (*i*) Trehoux *et al.* (1988); (*j*) Trehoux *et al.* (1977); (*k*) this work.

type compound $K_{0.88}(OH)_{0.69}H_{1.81}(H_2O)_{0.89}Nb_2O_6$ obtained, for the first time, by hydrothermal reaction.

2. Experimental

2.1. Synthesis, SEM/EDX, elemental analysis and thermogravimetry

Regular, octahedral, colorless, single crystals of $K_{0.88}(OH)_{0.69}H_{1.81}(H_2O)_{0.89}Nb_2O_6$ were obtained by hydrothermal reaction of Nb_2O_5 and KOH (with Nb_2O_5:KOH molar ratios of 1:7 or 1:8) in Teflon-lined autoclaves. Reaction temperatures from 453 to 513 K were used, and the reaction times ranged from 12 h to 3 d. A Jeol JSM-6500F was used for SEM (scanning electron microscopy) and EDX (energy-dispersive X-ray analysis). The crystals were dissolved in HF, and the elemental analysis for potassium was performed using a SHIMADZU AA-6800 atomic absorption spectrometer and the analysis for Nb was performed using a HITACHI P-4010 inductively coupled plasma emission spectrometer. Thermogravimetry (TG) and differential thermal analysis (DTA) data in the temperature range 300 to 1073 K were collected in air using a Rigaku Thermoflex apparatus and a heating rate of 2 K min^{-1}.

2.2. Single-crystal X-ray data collection, structure solution and refinement

An approximately 0.10 × 0.10 × 0.10 mm single crystal was mounted on a glass fiber or placed into a homemade sealed capillary holder and measured, using graphite-monochromated Mo $K\alpha$ radiation, on a Rigaku AFC7R diffractometer with a rotating-anode generator. The data in the temperature range 173–373 K were collected with a temperature variance of ±1 K using the ω–2θ scan technique to a maximum 2θ value of 89.2°. The computer-controlled slits were set to 3.0 mm (horizontal) and 3.0 mm (vertical). No decay correction was applied. Further details of the single crystal experiment are found in Table 2.[1] The structure was solved by the *SHELX*97 (Sheldrick, 1990) direct method and expanded using Fourier techniques (Beurskens *et al.*, 1999). Further details of the X-ray data collection and the crystal structure solution and refinement are listed in Table 2. Neutral atom scattering factors were taken from Cromer & Waber (1974), and anomalous dispersion effects were included in F_{calc} (Ibers & Hamilton, 1964). The values for $\Delta f'$ and $\Delta f''$ were those of Creagh & McAuley (1992), the values for the mass attenuation coefficients were those of Creagh & Hubbell (1992), and all calculations were performed using the *CrystalStructure* software package (Rigaku/MSC, 2000–2004; Watkin *et al.*, 1996).

2.3. Powder data collection, structure determination, refinement and validation

Synchrotron measurements were made using the BL02B2 beamline at the SPring-8 facility (Hyogo Prefecture, Japan).

[1] Supplementary data for this paper are available from the IUCr electronic archives (Reference: BP5032). Services for accessing these data are described at the back of the journal.

Table 2
Details of $K_{0.88}(OH)_{0.54}H_{1.66}(H_2O)_{1.04}Nb_2O_6$ structure determined from single-crystal X-ray data.

For all structures: $KNbO_3$, M_r = 180.00, cubic, $Fd\bar{3}m$, Z = 4. Experiments were carried out with Mo $K\alpha$ radiation using a Rigaku AFC7R diffractometer. Refinement was on 12 parameters.

	173 K	300 K	373 K
Crystal data			
a (Å)	10.635 (4)	10.645 (4)	10.665 (8)
V (Å^3)	1202.8 (8)	1206.2 (7)	1212 (1)
μ (mm^{-1})	1.29	1.29	1.28
Crystal size (mm)	0.10 × 0.10 × 0.10	0.20 × 0.20 × 0.20	0.20 × 0.20 × 0.20
Data collection			
$x(O^{48f})$	0.3136 (7)	0.3113 (6)	0.3102 (6)
Frac.(K^{16d})	0.71 (2)	0.72 (2)	0.67 (1)
$U^{11} = U^{22} = U^{33}$ (K^{16d})	0.024 (2)	0.032 (3)	0.037 (3)
$U^{11} = U^{22} = U^{33}$ (Nb^{16c})	0.0213 (8)	0.0204 (7)	0.0207 (6)
$U^{11} = U^{33}$ (O^{48f})	0.009 (2)	0.010 (2)	0.009 (2)
U^{22} = (O^{48f})	0.012 (4)	0.004 (3)	0.004 (3)
$U^{11} = U^{22} = U^{33}$ (O_{aq}^{8b})	2.0 (7)	0.37 (5)	0.38 (4)
No. of measured, independent and observed [$F^2 > 2.0\sigma(F^2)$] reflections	373, 344, 154	352, 325, 143	352, 325, 131
R_{int}	0.041	0.050	0.045
Refinement			
$R[F^2 > 2\sigma(F^2)]$, $wR(F^2)$, S	0.043, 0.060, 1.83	0.042, 0.058, 1.76	0.042, 0.046, 1.95
No. of reflections	344	325	325
$\Delta\rho_{max}$, $\Delta\rho_{min}$ (e Å^{-3})	13.20, −22.40	25.20, −12.40	25.40, −33.80

Table 3
Data collection and refinement details for $K_{0.88}(OH)_{0.54}H_{1.66}(H_2O)_{1.04}Nb_2O_6$.

Radiation type	Synchrotron	Neutron
Symmetry	Cubic	
Space group	$Fd3m$	
Z	8	
Formula weight	1383.31	
a (Å)	10.6454 (1)	10.6551 (2)
V (Å^3)	1206.39 (1)	1209.69 (1)
d_x (g cm^{-3})	3.82	3.82
Instrument	BL02B2 (SPring-8)	HERMES (Tohoku Uni.)
Wavelength	0.77703	1.8265
Temperature (K)	300	300
Container material	Quartz	Vanadium
2θ range (°)	2–40	10–156
2θ step (°)	0.01	0.1
No. of reflections	74	56
No. of variables	16	22
Profile function	Pseudo-Voigt	Pseudo-Voigt
U	0.0106 (5)	0.39 (1)
V	−0.0040 (1)	−0.44 (2)
W	0.0015 (1)	0.260 (7)
Agreement factors		
R_p	0.0287	0.0208
R_{wp}	0.0464	0.0270
R_{Bragg}	0.0481	0.0678
R_f	0.0342	0.0573
χ^2	3.60	0.0244

After the sample powder was carefully ground, the coarse fraction was separated by precipitation and the fine fraction was packed into a quartz capillary 0.1 mm diameter. The diffraction data were collected with a constant wavelength (λ = 0.77742 Å) at temperatures ranging from 300 to 773 K. The neutron data at λ = 1.8265 Å were collected, with the sample housed in a cylindrical vanadium container, using the Hermes diffractometer at the Japan Atomic Energy Agency's JRR-3 reactor (Tokai, Japan). The crystal structure was initially determined using the *FOX* program (Favre-Nicolin & Černý, 2002), and the final refinement was carried out with *FULLPROF* and *Winplotr* software (Rodriguez-Carvajal, 1990). The room-temperature data collection and refinement details are summarized in Table 3. The bond-valence calculations were performed according to the Brown method using *VaList* software (Rodriguez-Carvajal, 1990).

2.4. Electrical measurements

The powder was carefully ground with water in an agate mortar, dried at 343 K, and uniaxially pressed in a stainless steel mould to form discs approximately 16 mm in diameter and 0.5 mm thick that were then polished before indium, silver or graphite electrodes were deposited on them. The relative density of the discs achieved by cold-pressing was ∼ 80%. The discs were positioned in a cell mounted in an electrical furnace and their impedance in the frequency range from 10 Hz to 1 MHz was measured at temperatures between 473 and 773 K using a HIOKI Chemical Impedancemeter controlled by a personal computer *via* a LabView interface.

3. Results and discussion

3.1. Crystal structure and chemical composition

EDX studies confirmed that the crystals contained no heavy cations other than potassium and niobium. According to the weight loss observed by TG/DTA (thermogravimetry/differential thermal analysis) measurements (see §3.2), the crystal structure of the new niobate includes water. When knowing the structure is of the pyrochlore type and assuming there are

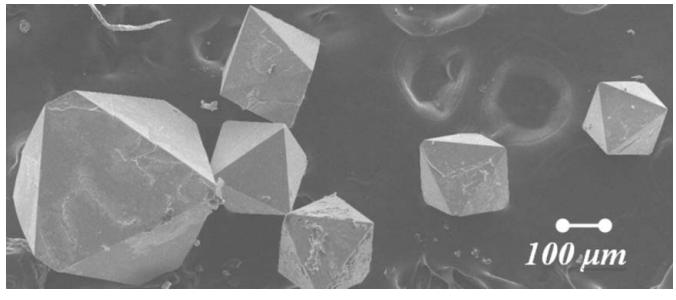

Figure 1
SEM photograph of $K_{0.88}Nb_2O_{7.58}H_{4.28}$ single crystals.

Table 4
Crystal structure and refinement details as obtained from high-resolution synchrotron powder X-ray data.

T (K)	300	373	473	573	673	773
a (Å)	10.6454 (1)	10.6489 (1)	10.6508 (1)	10.6412 (1)	10.6247 (1)	10.6457 (1)
V (Å^3)	1206.39	1207.57	1208.22	1204.92	1199.36	1206.49
ρ_{calc} (g cm^{-3})†	3.82	3.805	3.71	3.56	3.54	3.52
x(O^{48f})	0.3105 (2)	0.3105 (2)	0.3107 (2)	0.3113 (2)	0.3104 (4)	0.3092 (4)
x(O^{32e})	0.4297 (5)	0.4296 (5)	0.4331 (5)	0.4413 (7)	0.423 (1)	0.408 (2)
Frac. (O^{32e})	0.222 (–)	0.270 (0)	0.264 (0)	0.264 (0)	0.186 (6)	0.162 (6)
Frac. (O^{16d})	0.288 (–)	0.324 (0)	0.3 (0)	0.168 (0)	–	–
B_{iso} (K^{16d}) (Å^2)	0.84 (6)	1.04 (7)	1.42 (7)	1.71 (8)	4.9 (1)	6.2 (1)
B_{iso} (Nb^{16c})	0.93 (1)	0.97 (1)	1.10 (1)	1.27 (1)	1.40 (2)	1.23 (2)
B_{iso} (O$^{48f,\ 32e,\ 16d}$)	0.77 (5)	0.81 (6)	1.05 (6)	1.57 (6)	2.8 (1)	2.6 (1)
No. of reflections	74	74	74	77	77	77
No. of variables	17	17	17	17	17	17
R_p	0.0287	0.0296	0.0278	0.0254	0.0290	0.0312
R_{wp}	0.0464	0.0501	0.0485	0.0415	0.0496	0.0489
R_f	0.0481	0.0426	0.0422	0.0396	0.0571	0.0820
R_{Bragg}	0.0342	0.0299	0.0281	0.0326	0.0477	0.0821
χ^2	3.60	4.49	4.26	3.17	4.53	4.42

† The density values were calculated using the formula weight obtained by elemental analysis at 300 K minus weight loss according to TG/DTA data.

absorption spectroscopy and inductively coupled plasma emission spectroscopy, single crystals contain 9.98 (3)% potassium and 53.63 (8)% niobium by weight. So the potassium/niobium ratio is less than unity, the potassium content per formula unit is 0.88, and the chemical composition is $K_{0.88}Nb_2O_{7.58}H_{4.28}$, where amounts of oxygen and hydrogen are straightforwardly calculated from the system of two equations according to the weight percentages of Nb and K. The shape of the single crystals suggested high symmetry for the lattice (Fig. 1). Indeed, single-crystal and X-ray powder patterns (Figs. 2–4) were indexed with a cubic cell; based on the systematic absences of hkl: $h + k$, $k + l$, $h + l = 2n$ and $0kl$: $k + l = 4n$ and the successful solution and refinement of the structure, the space group was determined to be $Fd3m$ (No. 227).

no niobium vacancies in the rigid $NbO_{6/2}$ framework but that protons can substitute for potassium, one can express the general electroneutral formula unit of the compound as $K_xH_yNb_2O_6{\cdot}(H_2O)_z$ or $K_xH_yNb_2O_{6+z}$. Indeed, according to the results of quantitative elemental analysis by atomic

The results of the crystal structure determination from single-crystal X-ray diffraction data are listed in Table 2. Careful examination of synchrotron powder patterns revealed the presence of the forbidden 442 reflection at 300–573 K, but not at 673 or 773 K (Fig. 3) when the water in the structure is released (see below). The presence of the diffraction line with $h = 4n$, $k = 4n$, $l = 2n$ indicates that water O atoms are located in higher than 8*b* multiplicity sites 32*e* or 96*g*, explaining high displacement parameters found from single-crystal data. The lower-background synchrotron pattern allowed the refinement of the water shift from the 8*b* site to the 32*e* position at room temperature (Table 4). That is, oxygen from water is located nearly midway between the 8*b* and 16*d* sites, and slightly closer to the 8*b* sites. During the first refinement cycles only potassium was indicated in 16*d* sites; the atomic fraction was found to be less than unity, but the potassium content appeared higher than that determined by elemental analysis. Most probably, the hydroxide ion or water molecule randomly substituted for potassium in 16*d* sites. Finally, the potassium fraction was fixed according to chemical analysis data; the occupancies of niobium and framework oxygen were fixed

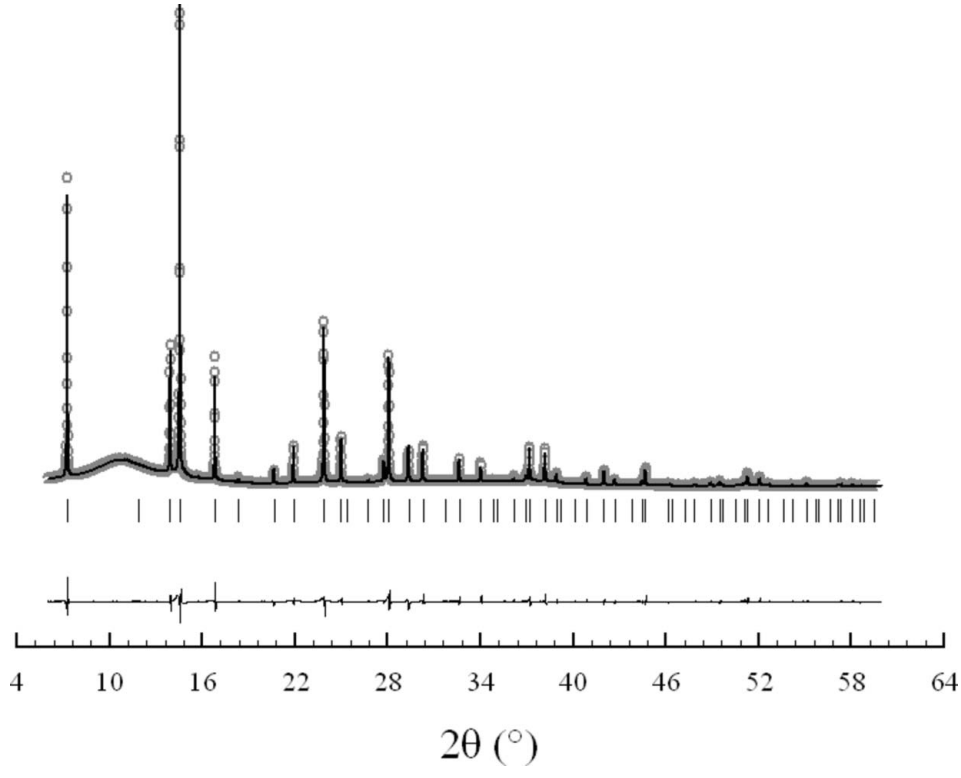

Figure 2
Example of Rietveld fit for $K_{0.88}Nb_2O_{7.58}H_{4.28}$ synchrotron powder pattern at 673 K. Circles indicate the observed pattern, the top line is the calculated pattern and the bottom line is the difference curve. Bars mark the positions of the Bragg peaks.

to unity, and only fractions of O atoms located in 16*d* and 32*e* sites were refined. The sum of the latter values at room temperature was fixed according to water content and at other temperatures was refined freely. At elevated temperatures ($\geq$ 373 K) the water oxygen fractions appeared somewhat high, probably because of high thermal motion and correlation with displacement parameters and atomic coordinates. The neutron diffraction pattern displayed a high background, indicating the presence of hydrogen in the lattice, which is considerably reduced on heating owing to water evaporation.

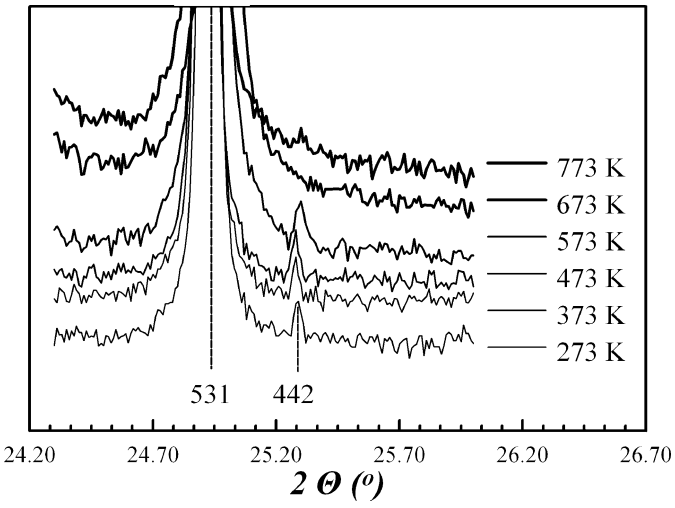

Figure 3
Synchrotron patterns in the area of the 442 reflection.

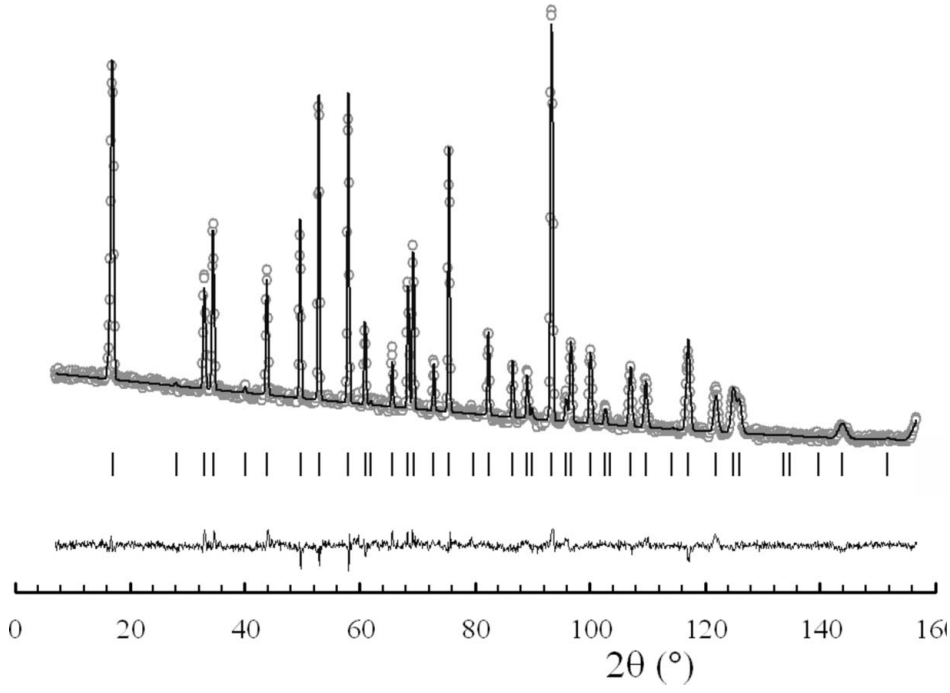

Figure 4
Rietveld plot for $K_{0.88}Nb_2O_{7.58}H_{4.28}$ neutron pattern at 300 K. Circles indicate the observed pattern, the top line is the calculated pattern and the bottom line is the difference curve. Bars mark the positions of the Bragg peaks.

The refinement performed in the present work allowed us to assign hydrogen to 96*g* sites (Table 5). Owing to their high mobility, the displacement parameters of potassium and hydrogen appeared to be large. The hydrogen locations are shown in Fig. 5 and selected interatomic distances are listed in Table 6. The K—O and Nb—O distances are in good agreement with the sums of ionic radii, 2.76 and 2.02 Å (Shannon, 1976). Niobium has six O atoms at equal distances, forming slightly distorted octahedron. The environment of the potassium comprises six O atoms in roughly planar 48*f* positions. The other two oxygen sites (32*e*) are located at the short distance of 1.28 Å and cannot be occupied simultaneously with the potassium site. The 32*e* oxygen sites have three hydrogen sites at a distance of $\sim$ 1.2 Å with the angle 100° between them, typical for a water molecule. The oxygen in 16*d* sites have six hydrogen sites $\sim$ 1.3 Å away, a distance slightly greater than the length of a covalent O—H bond in a water molecule, with an angle of $\sim$ 90° between the sites, corresponding to hydroxide ions. The hydroxide ions are bound to the framework O(48*f*) anions with hydrogen bonds of 1.68 Å. OH^- groups appeared to be fixed in the middle of the cavities in 16*d* sites because of the repulsion between the electron densities of O(48*f*)$\cdots$H hydrogen bonds and also between the lone pairs of O(48*f*) atoms, while similar repulsive interactions shift water molecules to 32*e* sites. The justification for the elongated O—H bonds and distorted geometries originates from the correlations between covalent O—H bond lengths and hydrogen O$\cdots$H bond lengths. The former are longer when the latter are shorter, therefore, considering the lone pairs of oxygen as extremely short bonds, the longer covalent O—H bonds and smaller H—O—H angles look natural. This leads to the conclusion that the H—O—H angle of 104° in pure water is mainly due to the presence of hydrogen bonding, while in the absence of hydrogen bonds the angle is further compressed because of the repulsion with lone pairs. According to the electroneutrality balance, there are plenty of 'free protons' not forming OH^- or water groups, but are hydrogen-bonded to the framework oxygen ions at 1.68 Å, most probably due to the hydrothermal conditions during synthesis.

Finally, the structural formula of the compound reads as $(K_{0.88}(OH)_{0.54})H_{1.66}(H_2O)_{1.04}Nb_2O_6$. An exhaustive check for all the available pyrochlore-type structures (to be reported elsewhere) showed that the present combination of potassium, water and hydroxide ions provides a new example of pyrochlore-type crystallographic arrangement. Comparison with

Table 5
$K_{0.88}Nb_2O_{7.58}H_{4.28}$ positional and displacement parameters obtained from neutron data.

The oxygen fractions in 32*e* and 16*d* sites are refined with their sum fixed according to the composition.

Atom		*x*	*y*	*z*	B_{iso} (Å^2)	Frac.
Nb	16*c*	0	0	0	1.23 (5)	1.0 (–)
O1	48*f*	0.311 (1)	0.125	0.125	0.26 (3)	1.0 (–)
K	16*d*	0.50	0.5	0.5	0.5 (2)	0.44 (–)
O2	16*d*	0.5	0.5	0.5	8.50 (2)	0.276 (–)
O3	32*e*	0.4306 (7)	0.4306 (7)	0.4306 (7)	3.4 (3)	0.258 (–)
H	96*g*	0.545 (1)	0.4196 (7)	0.4196 (7)	13.1 (5)	0.357 (–)

Table 6
Selected interatomic distances and angles calculated from $K_{0.88}Nb_2O_{7.58}H_{4.28}$ crystal structure refinement results obtained using neutron data.

	l (Å)		α(O) (°)
K—O × 6	2.761 (9)	H—O16*d*—H × 6	93.0 (6)
Nb—O × 6	1.991 (4)	H—O16*d*—H × 6	87.0 (6)
O48*f*—H × 2	1.68 (2)	H′—O32*e*—H′ × 3	100.3 (9)
O16*d*—H × 6	1.30 (1)	H″—O32*e*—H″ × 3	112.9 (6)
O32*e*—H′ × 3	1.23 (1)	H′—O32*e*—H″ × 6	123.5 (8)
O32*e*—H″ × 3	1.94 (1)	H′—O32*e*—H″ × 3	43.3 (7)

other niobium-containing pyrochlore structures shows that the distortion of niobium polyhedra specified by the *x*(32*e*) atomic coordinate is almost the same for AB_2O_6, deficient $A_2B_2O_6$ and hydrated $A_2B_2O_6{\cdot}nH_2O$ pyrochlores, but it is larger for classic pyrochlores $A_2B_2O_7$ (in particular reduced to Nb +4.5; Istomin *et al.*, 1997) containing additional O atoms in the cages in 8*b* sites (Table 1). This may lead to the conclusion that the distortion of NbO_6 octahedra is primarily determined by the oxidation state of niobium. It is important to note that all the typical representatives of pyrochlores in which deuterium sites have been determined contain water molecules in 32*e* sites, whereas alkali ions are mainly located in 16*d* sites (Table 1).

Exploring all the available crystal structure information [Inorganic Crystal Structures Database (ICSD) database, FIZ Karlsruhe; Crystallography Open Database (COD), Le Mans] for the framework structures containing *charge-balancing acidic protons*, similar to the compound described in the current work, one may note they are mainly represented with acidic sulfates, phosphates, arsenates or the related acidic salt (Troyanov *et al.*, 2004; Alaoui Tahiri *et al.*, 2002; Catti *et al.*, 1980). One should note that these structures usually contain hydrogen covalently bonded to oxygen at a distance of less than 1 Å, thus these H atoms are not considered as '*free protons*'. One example is the crystal structure of the compound $Cs_3(HSO_4)_2(H_{1.5}P_{0.5}S_{0.5}O_4)$ (Haille *et al.*, 1998), where acidic hydrogen provides fast ionic transport. The structure comprises O—H bonds of length 1.15–1.3 Å,which is somewhat longer than the O—H bonds in liquid water and in other phosphates and sulfates. Another structural family of fast protonic conductors, oxide-ion deficient perovskites, contains fewer mobile 'free' protons owing to the water absorbtion from an environment. According to neutron diffraction experimental results (Sata *et al.*, 1996; Ahmed *et al.*, 2008; Ito *et al.*, 2007), the protonic sites are located at approximate distances 0.9–1.2 Å to the framework oxide ions. In particular, the $SrTi_{0.98}Sc_{0.02}O_3$ crystal structure hosts about 2 mol % of hydrogen with each proton bonded to two oxide ions with a distance of 1.2 Å (Sata *et al.*, 1996). The O—H bond lengths reported in the present paper are similar to those found in perovskites and in $Cs_3(HSO_4)_2(H_{1.5}P_{0.5}S_{0.5}O_4)$, while the longer distances between framework oxide ions and 'free' protons are explained with higher hydrogen content, different structure geometry comprising two hydrogen sites at 1.68 Å to

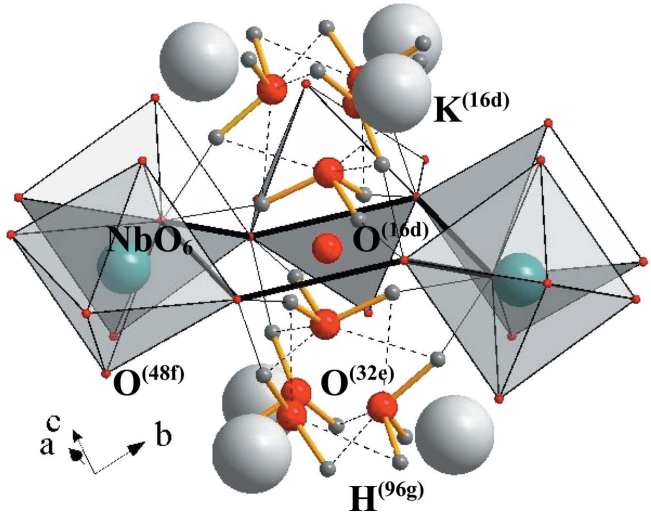

Figure 5
Protons location in the $K_{0.88}Nb_2O_{7.58}H_{4.28}$ structure. Thin lines represent hydrogen bonds of 1.68 Å, dashed lines represent distances of 1.9 Å.

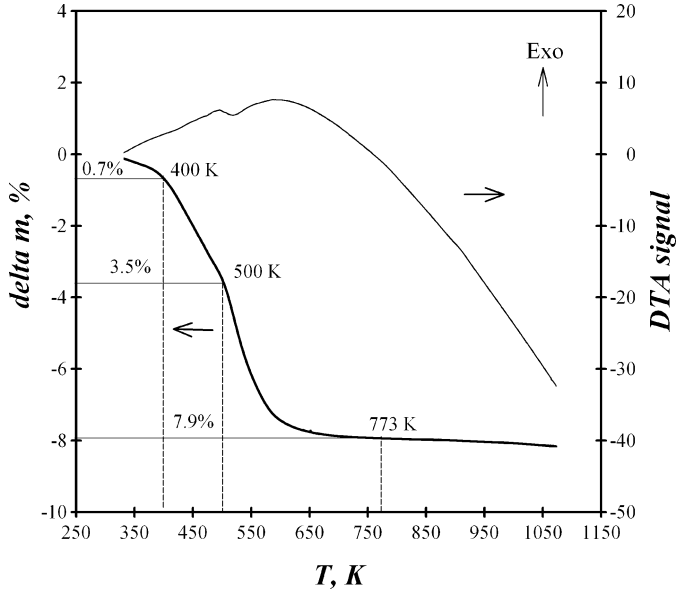

Figure 6
TG and DTA curves of $K_{0.88}Nb_2O_{7.58}H_{4.28}$.

each framework oxide ion and H—O—H angles, $\simeq 50^\circ$, much smaller than in perovskite structures, 90° (Ahmed *et al.*, 2008).

3.2. Thermal properties

Three different stages of weight loss are observed in the TG curve of $K_{0.88}(OH)_{0.54}H_{1.66}(H_2O)_{1.04}Nb_2O_6$, 0.7%, 2.8% and 4.3% (Fig. 6), but only one clear endothermic peak at around 523 K could be detected by DTA analysis. The first shoulder in the TG curve corresponds to the evaporation of weakly absorbed surface water. The appearance of two shoulders at higher temperatures confirms the presence of water species and hydroxide ions in the structure. According to the presence of the 442 reflection in powder patterns collected at 300–573 K, the second shoulder on the TG curve is thought to correspond to the evaporation of hydroxide ions from 16*d* sites together with protons forming water, and the last stage of weight loss should correspond to water escaping from 32*e* sites. The suggested model shows excellent agreement between the results of the thermogravimetric studies and the hydroxyl group, and water content calculated from 16*d* and 32*e* oxygen site occupancies at room temperature. That is, according to the X-ray data, OH^- located in 16*d* sites plus an appropriate amount of protons together make up exactly 2.8% of the formula weight and the total water content according to the chemical analysis is 8.2%. The overall weight loss up to 800 K is $\sim 8\%$, so TG and DTA data suggest that no water loss accompanied by oxygen release from the $NbO_{6/2}$ pyrochlore framework occurs and therefore oxygen vacancies in NbO_6 octahedra are not expected to be created, contrary to other protonated pyrochlore-type compounds, particularly those containing tungsten (Kumada *et al.*, 1985). This discrepancy can be explained by local bond-valence balance which is restricted by the stability of niobium oxidation state +5 and the coordination preference towards an octahedral environment, while the crystal chemistry of tungsten leaves more freedom for the oxidation state and coordination. Since the weight loss is limited to water and hydroxyl group content, even at temperatures as high as 773 K the new crystal structure $(K_{0.88}(OH)_{0.54})H_{1.66}(H_2O)_{1.04}Nb_2O_6$ is expected to retain charge-balancing 'free protons' owing to the high stability of the $NbO_{6/2}$ framework. This assumption agrees well with the *in-situ* powder neutron data at 800 K which fits better when hydrogen is included in the structural model. According to X-ray phase analysis of the powder annealed at 873 K, either a phase segregation or phase transition to lower symmetry occurs between 773 and 873 K. The change in the cell parameter with increasing temperature is shown in Fig. 7. At 173–673 K the cell parameter change is a result of two competitive processes: an increase owing to thermal expansion and a contraction owing to the release of water. For much smaller particles studied by synchrotron diffraction, the water release is much faster and the cell parameter change is therefore smoother. At 673 K all the water has been released and further heating results in thermal expansion of the lattice.

Despite the discontinuous change in cell parameters seen with increasing temperature, the density (calculated from the formula weight obtained by elemental analysis minus the water inferred from the TG/DTA data) decreases continuously over the same temperature range. Like the change in cell parameter, changes in O-atom coordinates (Fig. 8) are related to the thermodynamics of water release. Up to 573 K the O-atom coordinates in a 32*e* site increase, bringing that site closer to a 16*d* site, while at higher temperatures the opposite trend is seen. The O-atom coordinates in a 48*f* site are almost constant at temperatures between 300 and 573 K, while at higher temperature they decrease and distort the niobium polyhedra.

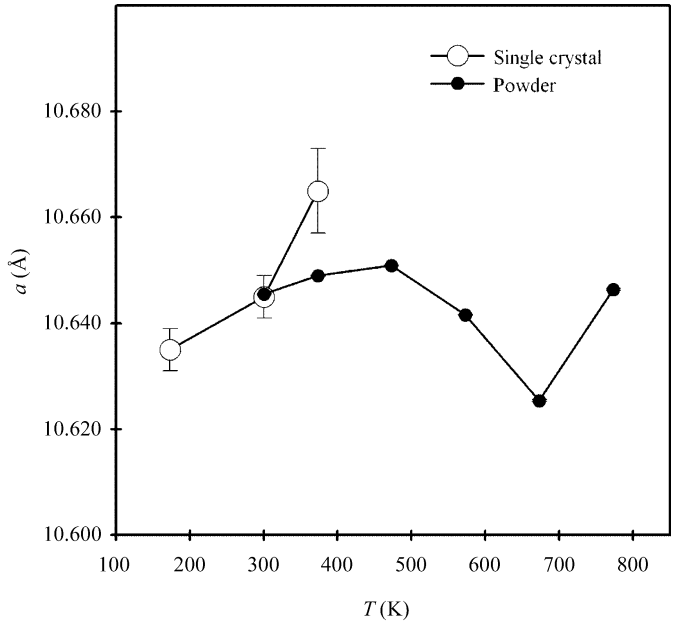

Figure 7
Temperature dependence of $K_{0.88}Nb_2O_{7.58}H_{4.28}$ cell parameters extracted from single-crystal and synchrotron powder X-ray diffraction data.

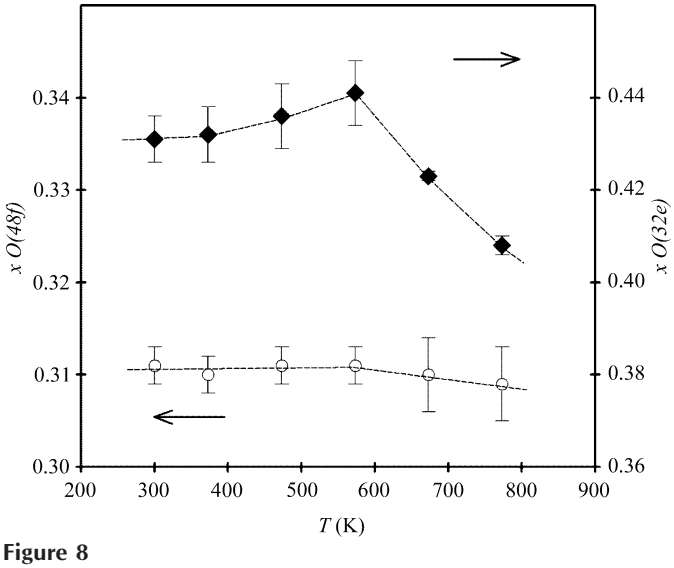

Figure 8
Relation between temperature and the coordinates of O atoms in the $K_{0.88}Nb_2O_{7.58}H_{4.28}$ crystal structure.

3.3. Electrical properties

Proton transport in hydrated or ion-exchanged pyrochlores has been known for a long time and has been confirmed by ^{1}H MAS NMR studies (Binesh *et al.*, 1996) and impedance measurements with reversible hydrogen-injecting electrodes (Slade *et al.*, 1989; Hinrichs & Tomandl, 1998). The measurement procedures and results have already been discussed in one of our previous papers (Smirnova *et al.*, 2008). As there are three regions of water loss in the TG curve of $K_{0.88}Nb_2O_{7.58}H_{4.28}$, there are also three regions with different activation energies in the Arrhenius plot showing the temperature dependence of the conductivity of this compound (Fig. 9). The first region (up to 473 K) has a very low activation energy and can be attributed to the conductivity owing to surface water condensed on the crystallites. The conductivity in the second region (473–62 K) can be attributed to either potassium ions moving or protons hopping, and protons riding on water molecules. As the activation energy is not influenced by water escaping from the 16 sites seen in this temperature range, and K^+ H_3O^+ does not seem to contribute significantly to this conduction, otherwise the free volume increase in the tunnels would improve transport. The conductivity in the last stage (623–773 K) shows a saturation-like small curve slope probably because of the water evaporation as it can significantly assist protons hopping. It can be concluded that the transference number for potassium is negligible because at this stage the conductivity does not increase with temperature. At 623 K the bulk conductivity reaches the 10^{-2} S cm^{-1} necessary for a 15 µm-thick film for a solid-oxide fuel cell (SOFC), while the total conductivity is still 10^{-4} S cm^{-1}. The boundary conductivities of cold-pressed compacts, however, decrease when the compacts are heated in non-humidified air for a long time. We did not test the material in humid atmospheres, and we think the role of boundaries might be positive when water condenses on them. Extended stability ranges with respect to both senses of temperature and water solubility suggest that the compound is a potential proton-conducting material for solid-oxide fuel-cell applications. In particular, the material is able to fill the gap (Norby, 2001) between hydroxide conductors (Poling *et al.*, 2006; helpful up to 550 K) or acidic sulfates (Haile *et al.*, 2001; helpful up to 500 K) and oxygen-deficient proton conductors (Steele & Heinzel, 2001; helpful at 773–973 K).

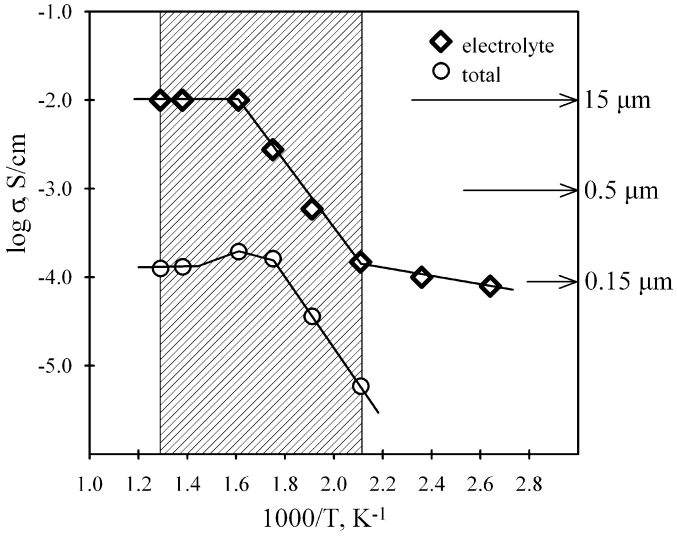

Figure 9
Arrhenius plot for the temperature dependence of the conductivity of a $K_{0.88}Nb_2O_{7.58}H_{4.28}$ disc (~ 20% porosity) in ambient air. The gap between utilization temperatures of SOFC solid electrolytes reported before is indicated by the shaded rectangle. The necessary conductivity values for SOFC solid electrolyte films of various thicknesses are marked with arrows (Smirnova *et al.*, 2008).

4. Conclusions

The new compound prepared by hydrothermal reaction, $K_{0.88}(OH)_{0.54}H_{1.66}(H_2O)_{1.04}Nb_2O_6$, has a pyrochlore-type crystal structure [*Fd*3*m*, a = 10.645 (4) Å at 300 K] with a novel arrangement of water molecules, OH^- groups and potassium atoms. Single-crystal and synchrotron powder X-ray diffraction studies revealed that most of the water is in 32*e* sites midway between 16*d* sites and 8*b* sites [x = 0.431 (5) at 300 K], that K atoms and hydroxyl groups are in 16*d* sites, and that protons are located in 96*g* sites. The presence of water molecules and hydroxide ions corresponds to two stages of weight loss evident in the TG curve. According to the weight loss observed up to 773 K, no oxygen vacancies are created in the $NbO_{6/2}$ framework, *i.e.* the structure should retain protons. This new compound might be useful for solid-oxide fuel-cell applications, filling the gap between low-temperature and high-temperature solid electrolytes because the bulk conductivity of a cold-pressed sample reaches 10^{-2} S cm^{-1} at 573 K.

Authors are thankful to Associate Professor Masaki Azuma (Kyoto University) for the beam time at SPring-8 and to Assistant Professor Takashi Saito (Kyoto University) for experimental support during synchrotron experiments.

References

Ahmed, I., Knee, ch. S., Karlsson, M., Eriksson, S.-G. Henry, P. F., Matic, A., Engberg, D. & Boerjesson, L. (2008). *J. Alloys Compd.* **450**, 103–110.
Alaoui Tahiri, A., Ouarsal, R., Lachkar, M., El Bali, B. & Bolte, M. (2002). *Acta Cryst.* E**58**, i91–i92.
Barnes, P. W., Woodward, P. M., Lee, Y.-J., Vogt, T. & Hriljac, J. A. (2003). *J. Am. Chem. Soc.* **125**, 4572–4579.
Beurskens, P. T., Admiraal, G., Beurskens, G., Bosman, W. P., de Gelder, R., Israel, R. & Smits, M. M. (1999). *DIRDIF*94. Crystallography Laboratory, University of Nijmegen, The Netherlands.
Binesh, N., Bhat, V. & Bhat, S. V. (1996). *Solid State Ionics*, **86–88**, 665–668.
Catti, M., Chiari, G. & Ferraris, G. (1980). *Bull. Miner.* **103**, 129–134.
Creagh, D. C. & Hubbell, J. H. (1992). *International Tables for Crystallography*, edited by A. J. C. Wilson, Vol. C, pp. 200–206. Boston: Kluwer Academic Publishers.
Creagh, D. C. & McAuley, W. J. (1992). *International Tables for Crystallography*, edited by A. J. C. Wilson, Vol. C, pp. 219–222. Boston: Kluwer Academic Publishers.

Cromer, D. T. & Waber, J. T. (1974). *International Tables for X-ray Crystallography*, Vol. 4. Birmingham: Kynoch Press.
Favre-Nicolin, V. & Černý, R. (2002). *J. Appl. Cryst.* **35**, 734–743.
Fourquet, J.-L., Plet, F. & de Pape, R. (1975). *Mater. Res. Bull.* **10**, 933–940.
Fourquet, J. L., Riviere, M., Le Bail, A., Nygrens, M. & Grins, J. (1988). *J. Solid State Inorg. Chem.* **25**, 535–540.
Fourquet, J.-L., Rousseau, M. & Pape, R. (1979). *Mater. Res. Bull.* **14**, 937–941.
Galati, R., Simon, C., Knee, C. S., Henry, P. F., Rainford, B. D. & Weller, M. T. (2008). *Chem. Mater.* **20**, 1652–1659.
Grins, J., Nygren, M. & Wallin, T. (1980). *Mater. Res. Bull.* **15**, 53–61.
Groult, D., Michel, C. & Raveau, B. (1975). *J. Inorg. Nucl. Chem.* **37**, 2203–2205.
Groult, D., Michel, C. & Raveau, B. (1982). *J. Solid State Chem.* **41**, 277–285.
Haile, S. M., Boysen, D. A., Chisholm, C. R. I. & Merle, R. B. (2001). *Nature*, **410**, 910–913.
Haille, S., Calkins, P. M. & Boysen, D. J. (1998). *Solid State Chem.* **139**, 373–387.
Hinrichs, R. & Tomandl, G. (1998). *Solid State Ionics*, **107**, 117–122.
Ibers, J. A. & Hamilton, W. C. (1964). *Acta Cryst.* **17**, 781–782.
Ikeda, S., Fubuki, M., Takahara, Y. K. & Matsumura, M. (2006). *Appl. Catal. A*, **300**, 186–190.
Istomin, S. Ya., D'yachenko, O. G., Antipov, E. V. & Svensson, G. (1997). *Mater. Res. Bull.* **32**, 421–430.
Ito, T., Nagasaki, T., Iwasaki, K., Yoshino, M., Matsui, T., Fukazawa, H., Igawa, N. & Ishii, Y. (2007). *Solid State Ionics*, **178**, 607–613.
Kramer, S., Spears, M. & Tuller, H. L. (1994). *Solid State Ionics*, **72**, 59–66.
Kumada, N., Ozawa, N., Kinomura, N. & Muto, F. (1985). *Mater. Res. Bull.* **20**, 583–589.
Lewandowski, J. T., Pickering, I. J. & Jacobson, A. J. (1992). *Mater. Res. Bull.* **27**, 981–988.
Murphy, D. W., Cava, R. J., Rhyne, K., Roth, R. S., Santoro, A., Zahurak, S. M. & Dye, J. L. (1986). *Solid State Ionics*, **18**, 799–801.
Norby, T. (2001). *Nature*, **410**, 877–878.
Poling, S. A., Nelson, C. R. & Martin, S. W. (2006). *Mater. Lett.* **60**, 23–27.
Rigaku/MSC (2000–2004). *Crystal Structure Analysis Package.* Molecular Structure Corporation, Texas, USA.
Riviere, M., Fourquet, J. L., Grins, J. & Nygren, M. (1988). *Mater. Res. Bull.* **23**, 965–975.
Rodriguez-Carvajal, J. (1990). *FULLPROF*. Abstracts of the Satellite Meeting on Powder Diffraction of the XV Congress of the IUCr, Toulouse, France, p. 127.
Rotella, F. J., Jorgensen, J. D., Biefeld, R. M. & Morosin, B. (1982). *Acta Cryst.* B**38**, 1697–1703.
Sata, N., Hiramoto, K., Ishigame, M., Hosoya, S., Niimura, N. & Shin, S. (1996). *Phys. Rev. B*, **54**, 15795–15799.
Shannon, R. D. (1976). *Acta Cryst.* A**32**, 751–767.
Sheldrick, G. M. (1990). *Acta Cryst.* A**46**, 467–473.
Slade, R. C. T., Hall, P. G. & Skou, E. (1989). *Solid State Ionics*, **35**, 29–33.
Smirnova, O., Kumada, N., Yonesaki, Y. & Kinomura, N. (2008). *Electrochem. Commun.* **10**, 485–487.
Steele, B. C. H. & Heinzel, A. (2001). *Nature*, **414**, 345–352.
Trehoux, J., Abraham, F. & Thomas, D. (1977). *J. Solid State Chem.* **21**, 203–209.
Trehoux, J., Abraham, F., Thomas, D., Doremieuz-Morin, C. & Arribart, H. (1988). *J. Solid State Chem.* **73**, 80–91.
Troyanov, S. I., Snigireva, E. M. & Ling, C. D. (2004). *Crystallogr. Rep.* **49**, 969–974.
Tuller, H. (1992). *Solid State Ionics*, **52**, 135–146.
Watkin, D. J., Prout, C. K., Carruthers, J. R. & Betteridge, P. W. (1996). *Crystals*. Chemical Crystallography Laboratory, Oxford, UK.